

Stresses in Silos

Dietmar Schulze

1. Introduction

Knowledge of the stresses acting in silos is important for many applications:

- Silo design for strength (e.g. DIN 1055 part 6 [1])
- Silo design for flow
- Loads on feeders and inserts
- Driving torque of feeders
- Design of silos in which a specific maximum stress is not exceeded (e.g. to avoid vibrations, particle attrition or extreme time consolidation)

The calculation methods used by an engineer who is interested in avoiding flow problems and in feeder design differ from the calculation methods of a civil engineer (e.g. DIN 1055 part 6 [1]) who is interested in the stability of the silo structure. The civil engineer would choose the parameters for calculating silo stresses so that the major part of the load from the bulk solid is carried by the silo walls, whereas the engineer who has to calculate the feeder load and the required driving power would assume that the silo walls carry only a minor part of the load of the bulk solid. The stress distribution across the periphery of the silo is another example of the different points of view: whereas a strong irregular distribution of the stresses on the silo wall is quite unimportant for the design of a feeder, these different stresses cannot be neglected for the structural design of the silo walls.

2 Stress calculation

2.1 The behaviour of bulk solids in silos

Figure 1 shows an element of bulk solid in a cylinder which is filled with bulk solid (frictionless walls). The element of bulk solid is affected by the vertical stress σ_v . As a result of the vertical stress, the horizontal stress σ_h acts in the horizontal direction. The stress ratio λ which is well-known from soil mechanics is used for the description of the ratio of σ_h to σ_v :

$$\lambda = \sigma_h / \sigma_v \quad (1)$$

Every bulk solid has a specific stress ratio λ . While an ideal, non-elastic solid has a stress ratio of 0, a fluid would have a stress ratio of 1. That of bulk solids stored at rest is mostly in the range from 0.3 to 0.6 .

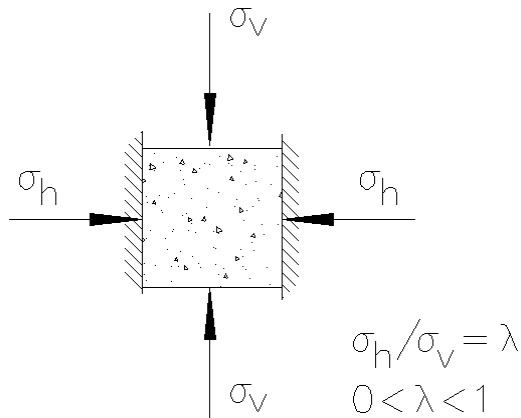


Figure 1: Element of bulk solid

For the stress calculation, a bulk solid is considered as continuum instead of single particles. Because of this the methods of continuum mechanics can be applied. If different sloped cuts through an element of bulk solid are considered it can be seen that different shear and normal stresses are acting at different cutting planes. This is shown in a simplified way in figure 1 where the stresses σ_h and σ_v which act in different directions differ from each other. In a bulk solid there is one direction where the maximum normal stress is acting. This maximum normal stress is called major principal stress σ_1 . The minimum normal stress which acts perpendicular to σ_1 is called minor principal stress σ_2 . Further information can be found in [2,4,5,7].

In contrast to a fluid, a bulk solid at rest can transmit shear stresses. While the pressure in a container filled with a fluid increases linearly with the depth (figure 2), the weight of the bulk solid in a silo is carried partly by the silo walls because of the shear stresses (friction at the silo wall) so that the stress does not increase linearly with the depth like the pressure of a fluid.

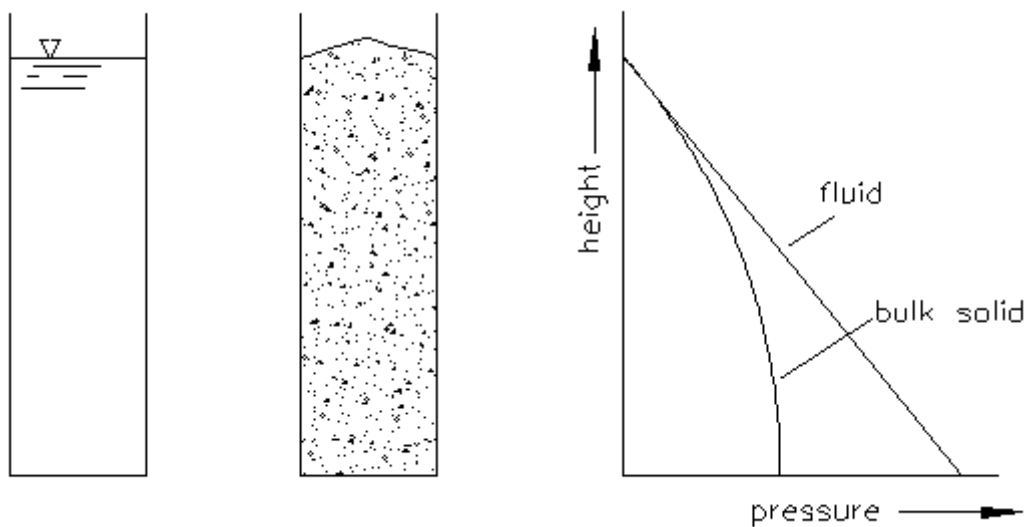


Figure 2: Pressures in fluids and stresses in bulk solids (in principle)

If an empty silo is filled, the plot of wall normal stress σ_w looks like figure 3.a [2]. The wall normal stress σ_w in the vertical part of the silo increases with depth, but with a decreasing gradient, tending asymptotically towards a maximum. In the vertical section of the silo the vertical stresses are the larger stresses while the horizontal stresses appear according to the stress ratio λ , equation (1). The major principal stress σ_1 acts downwards along the silo axis. As the silo walls are approached, the direction of the major principal stress diverges more and more from the vertical direction as it can be seen from the trajectories of the major principal stress, σ_1 , in figure 3.a.

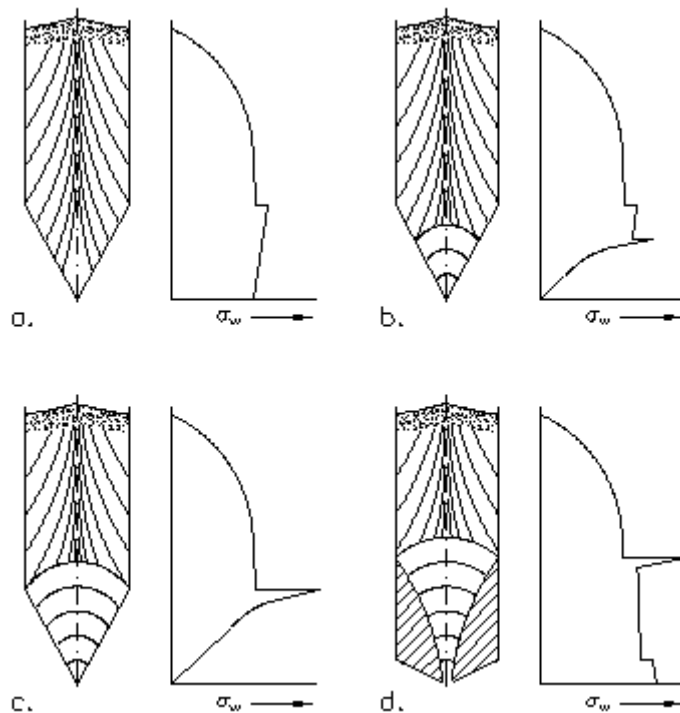


Figure 3: Qualitative courses of wall normal stresses, σ_w , and assumed trajectories of the major principal stress, σ_1 [2,3].

A point of discontinuity is present at the transition from the vertical section to the hopper. In the hopper the stress can decrease or first increase and then decrease on the way down through the hopper. This depends on the geometry of the hopper and the bulk solids properties. This stress state after the filling of the silo is called active stress state or filling state. As with the vertical section, in the active stress state the larger stresses in the hopper are also acting downwards (major principal stress acts vertically along the hopper axis).

At the beginning of discharge of a mass flow hopper all of the silos contents are set in motion and the stress conditions in the hopper change. Starting at the (theoretical) hopper apex the passive stress field (passive state of stress) prevails. When the bulk solid flows downwards through the converging hopper section, the bulk solid is compressed horizontally whereas the vertical stress is reduced due to the flow being directed downwards. Therefore, the stresses acting in the horizontal direction become the larger stresses (major principal stress acts horizontally in the hopper axis). In the case shown in figure 3.b, which shows the stresses just after the start of the discharge

the passive state of stress is only present in the lower part of the hopper whereas in case of figure 3.c (shortly after 3.b) the passive stress field has developed in the whole hopper. In the vertical part of the silo the active state of stress remains unchanged if no local convergences (local convergences caused by inserts, dents, etc.) are present. At the transition from the active to the passive stress field (in case of mass flow silos the transition from the vertical section to the hopper) a local stress peak occurs which is called the switch. The passive state of stress remains even if the discharge is stopped.

In the case of a funnel flow silo, the bulk solid flows downwards inside the dead zones. If the borderline between the flow zone and the dead zone intersects the silo wall as it is shown in figure 3.d, a stress peak (switch) is formed at that point. The position of the stress peak cannot be predicted so that the whole vertical section of the silo has to be designed to resist the stress peak.

While figure 3 shows the wall normal stress σ_w , in figure 4 the qualitative course of the vertical stress σ_v is shown for the active (figure 4.a) and the passive stress states (figure 4.b) in the hopper. Figure 4.a corresponds to figure 3.a and figure 4.b corresponds to figure 3.c. In the vertical section the course of the vertical stress σ_v is similar to the course of the wall normal stress σ_w . In the hopper the course of the vertical stress depends on the vertical stress at the transition from the vertical section to the hopper, the characteristics of the bulk solid and the geometry of the hopper. The curve in figure 4.a can be considered as one possible course. The vertical stress decreases rapidly with depth in the passive stress state where in the lower part of the hopper the vertical stress is proportional to the distance to the imaginary hopper apex. This course is called the radial stress field. The vertical stress at the outlet is independent from the vertical stress at the transition (in the case where the hopper is sufficiently high).

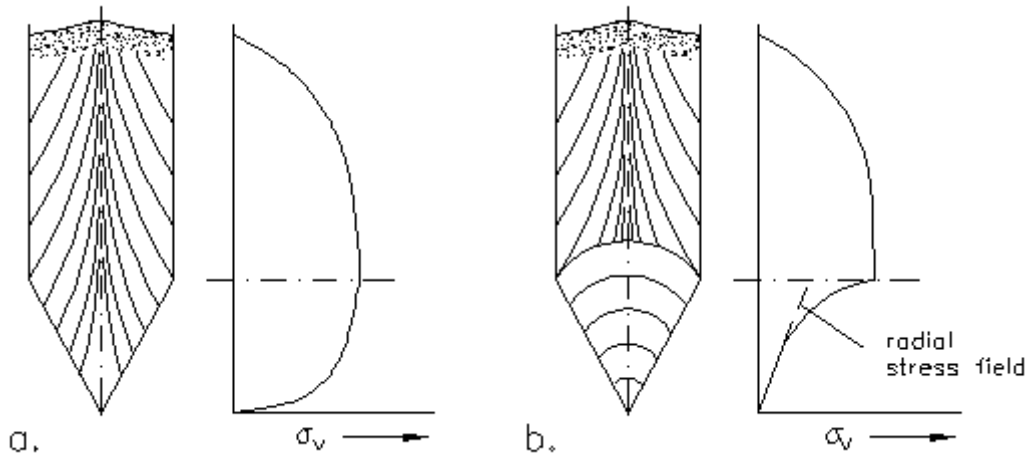


Figure 4: Qualitative course of the vertical stress σ_v , in the case of filling state (a) and in the case of emptying state (b) in a mass flow silo

Just after the filling of an empty silo (filling state, active stress state) the vertical stress at the outlet is larger than in the case of the passive stress state (discharging) [4,6-9]. In experiments stresses up to 10 times higher than in the case of the passive stress field have been measured for the active stress state [4,7]). Figure 5 shows what happens during the filling and discharging of a silo. During filling the filling height h_f and the

vertical stress at the outlet, σ_v , increase with time. As soon as bulk solid is discharged the first time the passive stress field develops and the vertical stress at the outlet, σ_v , decreases suddenly. Thus it can be shown that at the beginning of the discharge a feeder has to be able to move the bulk solid under a huge vertical stress σ_v . Therefore the feeder has to exert a large horizontal force F_h on the bulk solid (figure 5 bottom). As soon as the bulk solid is in motion the passive stress field with its low vertical stresses prevails thus reducing the feeder force F_h sharply.

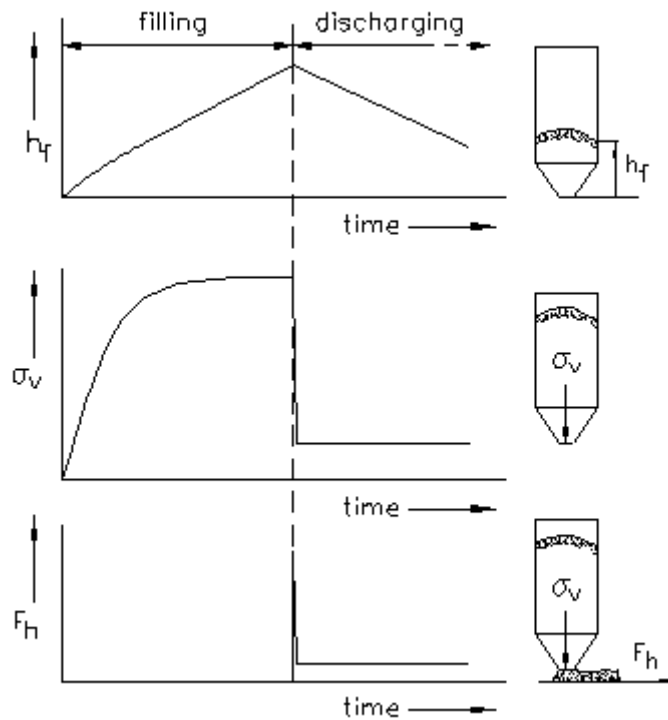


Figure 5: Filling height h_f , vertical stress at the outlet σ_v , and feeder force F_h vs. time

2.2 Methods of stress calculation (overview)

From the considerations above it can be seen that three different cases have to be taken into account when calculating stresses in silos:

- Stresses in the vertical part of silo
- Stresses in the hopper (active state of stress, filling state)
- Stresses in the hopper (passive state of stress, emptying state)

Stresses in silos have been investigated both experimentally and theoretically for approximately 100 years. At first the stresses in the vertical part of a silo were considered (Janssen [10], Koenen [11]). The hopper stresses were examined later. The best known investigations are those of Jenike [4,12], Walker [13,14] and Walters [15,16]. The first approaches are based on slice element methods where the equilibrium of forces on slice elements of infinitesimal thickness is considered (vertical section: [10,15], hopper: [13,14,16]).

The calculation method which was developed by Jenike [4,12] describes the hopper stresses for the passive stress state. Jenike's approach can also be used when designing silos for flow by determining the maximum hopper slope for mass flow and the minimum outlet size to prevent arching and ratholing. Jenike presented the results of his calculations in the form of diagrams to simplify the application of his method.

More recent investigations are from Enstad [17] and Benink [18]. They calculated the stresses in the hopper for the passive stress state with the aid of slice element methods. The work of Motzkus [19] must also be mentioned when dealing with the calculation of the hopper stresses at filling (active stress state). Motzkus identified the fact that some of the assumptions of Walker and Walters were not realistic and, therefore, he introduced improved assumptions. The slice element method for the calculation of the hopper stresses at filling derived by Schulze [7] considers the compressibility of the bulk solid.

The most recent investigations use the finite element method (FEM) for the stress calculation where the material properties are specified by material models (called material law). The material laws describe the dependency of the stresses in a bulk solid on the deformation (an example for a material law is Hooke's law).

In addition to Jenike's diagrams which are used for the calculation of stresses in the hopper in the passive stress state and for silo design for flow, the slice element methods are applied as standard practice, since they are easy to use. Several standards [1,23,24] for the structural design of silo walls are based on Janssen's approach [10]. Motzkus' slice element method [7,19] provides useful results for the calculation of stresses in the hopper after filling (active state of stress). Enstad's approach [17] can be applied for the emptying state (passive stress state).

This essay describes how to determine the stresses in the vertical part of a silo according to the approach of Janssen [10]. This method is also applied in the program SSTOOL [44], with which stresses in silos and containers can be assessed.

2.3 Calculation of the stresses in the vertical section of a silo

The stresses in the vertical section of a silo (active state of stress) have been calculated by Janssen [10], who used a so-called slice element method. He considered a slice-shaped volume element of infinitesimal height dz (figure 6) which has the same cross-sectional area A as the vertical section of the silo. Assuming constant vertical stress σ_v and constant bulk density ρ_b across the whole cross-section, the equilibrium of forces in z -direction yields:

$$A\sigma_v + \rho_b A dz = A(\sigma_v + d\sigma_v) + \tau_w U dz \quad (2)$$

After the introduction of the wall friction angle

$$\tan \varphi_1 = \tau_w / \sigma_w \quad (3)$$

and the stress ratio (s. section 2.1)

$$\lambda = \sigma_h / \sigma_v \quad (4)$$

an ordinary differential equation for the vertical stress σ_v is obtained.

$$\frac{d\sigma_v}{dz} + \sigma_v \lambda \frac{U}{A} \tan \varphi_x = g \rho_b \quad (5)$$

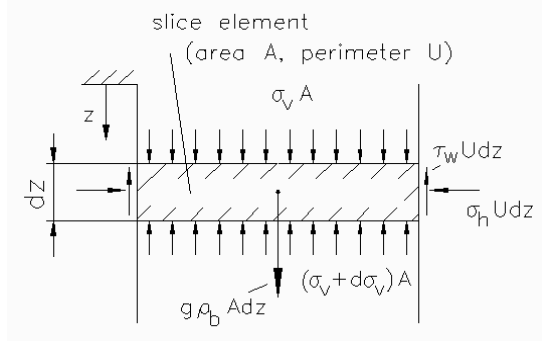


Figure 6: Slice element in the vertical section

From the integration of the differential equation (5) whilst considering the boundary condition that the vertical stress is equal to σ_{v0} at $z = 0$ it follows that:

$$\sigma_v = \frac{g \rho_b A}{\lambda \tan(\varphi_x) U} \left\{ 1 - e^{-\frac{\lambda \tan(\varphi_x) U z}{A}} \right\} + \sigma_{v0} e^{-\frac{\lambda \tan(\varphi_x) U z}{A}} \quad (6)$$

For $\sigma_{v0} = 0$ it follows from eq. (6) that:

$$\sigma_v = \frac{g \rho_b A}{\lambda \tan(\varphi_x) U} \left\{ 1 - e^{-\frac{\lambda \tan(\varphi_x) U z}{A}} \right\} \quad (6.a)$$

Horizontal stress σ_h and wall shear stress τ_w can be calculated by combining eqs. (3), (4), and (6):

$$\sigma_h = \frac{g \rho_b A}{\tan(\varphi_x) U} \left\{ 1 - e^{-\frac{\lambda \tan(\varphi_x) U z}{A}} \right\} + \lambda \sigma_{v0} e^{-\frac{\lambda \tan(\varphi_x) U z}{A}} \quad (6.b)$$

$$\tau_w = \frac{g \rho_b A}{c} \left\{ 1 - e^{-\frac{\lambda \tan(\varphi_x) U z}{A}} \right\} + \lambda \tan(\varphi_x) \sigma_{v0} e^{-\frac{\lambda \tan(\varphi_x) U z}{A}} \quad (6.c)$$

The e-function in eqs. (6) to (6.c) approaches zero for large values of z . Therefore, the expression in front of the term in brackets is the stress which is approached for large values of z , i.e. in case of a silo with sufficiently large height/diameter ratio.

The expression in front of the brackets depends on the bulk solid properties and the silo geometry represented by the ratio A/U (cross-sectional area A divided by perimeter U). In case of a cylindrical silo, the ratio A/U is equal to $d/4$ (d = silo diameter). Therefore, the maximum stress which is possible is proportional to the diameter of the vertical section of the silo (see eqs. (6.a) to (6.c)). For this reason, silos are usually slender

(small d) and high. In contrast to this, fluid containers (e.g. oil tanks) are usually flat and have a large diameter because of the hydrostatic pressure.

The validity of the Janssen equation (6.a) has been checked in several experimental tests over the last 100 years, e.g.[2,25-27]. For example, the influence of the wall friction angle φ_x is as follows: A rough wall (= large wall friction angle) carries a larger part of the weight of the bulk solid than a smooth wall (= small wall friction angle) . Therefore, the maximum horizontal stress is greater in a silo with a smoother wall (if all other parameters and dimensions are identical). This can be seen clearly in eq.(6.b) where the wall friction angle φ_x is placed in the denominator of the first term.

The Janssen equation is the basis of several standards for the calculation of stresses in silos because of its principle validity (e.g. [1,23,24]). Janssen determined the value of the stress ratio λ by adapting equation (6) to the stresses measured in a model silo.

Often the equation of Kézdi [28] is used for the estimation of the stress ratio λ :

$$\lambda = 1 - \sin \varphi \quad (7)$$

φ is the bulk solids angle of internal friction. Usually, the effective angle of internal friction, φ_e , measured in a shear tester is often used in its place. The German standard DIN 1055 part 6 (loads in silo cells) [1] recommends the following equation which is based on eq. (7):

$$\lambda = 1.2(1 - \sin \varphi) \quad (8)$$

The use of eq. (8) results in higher wall loads in the upper area of the silo, i.e. wall normal stresses σ_w and shear stresses τ_w are greater than those calculated on the basis of eq. (7). Therefore, the load assumptions for the structural design are on the safe side with eq.(8). To be on the safe side for applications where the maximum vertical stress is important (e.g. for the calculation of the feeder load or the maximum vertical stress) the smaller λ (eq.(7)) should be used because it yields higher vertical stresses.

For rough estimations of the stresses in the vertical section the following value of λ can be used [8,29].

$$\lambda = 0.4 \quad (9)$$

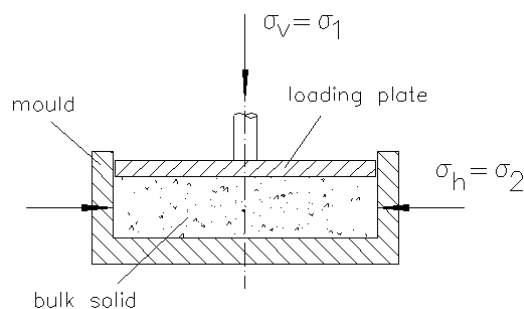


Figure 7: Uniaxial compression in the lambda-meter [30,33,34]

The values of the stress ratio which are calculated according to eq. (8) and DIN 1055 part 6 [1], respectively, are not correct in any case because the stress ratio depends on a lot of parameters which are not taken into account in eq.(8). A step towards improving safety is the recommendation in the new ISO-guideline [30] to determine the stress ratio directly from a uniaxial compression test with a modified oedometer (figure 7). This kind of test was used by Lohnes [31] and Kwade et al. [33,34] and recommended by Nielsen and Kolymbas [32]. The test is performed in the following way: A cylindrical mould is filled with the bulk solid to be tested. Then a vertical stress is applied on the sample and the resulting horizontal stress is measured. This test does not take into account all influencing parameters, but all which depend on the properties of the bulk solid. Measurements show that it is possible to use a modified oedometer - called a lambdameter - to determine the stress ratio λ [33,34].

2.4 Calculation of the hopper stresses

The stresses in the hopper can be assessed also using a slice element method. An equilibrium of forces on a slice element in the hopper (figure 8) yields the following equation [7,16,19,40]:

$$d(A\sigma_v) + g_c A dz = \sin(\Theta) \sigma_w dA_M + \cos(\Theta) \tau_w dA_M \quad (10)$$

Please note the different direction of co-ordinate z compared to the vertical section.

If fully mobilized wall friction is assumed (see eq.(3)), it follows:

$$\frac{d\sigma_v}{dz} - n \frac{\sigma_v}{z} = -g_c \quad (11)$$

with:

$$n = (m+1) \left\{ K \left[1 + \frac{\tan(\mu_w^2)}{\tan(\Theta)} \right] - 1 \right\} \quad (12)$$

$$K = \sigma_w / \sigma_v \quad (13)$$

With the parameter m the shape of the hopper is taken into account: $m = 0$ for wedge-shaped hoppers, $m = 1$ for conical hoppers.

At wedge-shaped hoppers with a small length to width ratio also the end walls play a role. If the friction at the end walls is taken into account, the differential equation (11) has to be extended by one additional term [7]:

$$\frac{d\sigma_v}{dz} - n \frac{\sigma_v}{z} - (1-m) \lambda \sigma_v \frac{2 \tan(\mu_w^2)}{l_s} = -g_c \quad (11.a)$$

Here λ_s is the ratio of the normal stress acting on the end walls to the mean vertical stress. As an approximation, the stress ratio λ_s is assumed to be equal to the stress ratio λ (eq.(4)). l_s is the length of the wedge-shaped hopper.

The values of K and n , respectively, are dependent on the the flow properties, the hopper geometry, and the mode of operation (filling, discharging). Thus the problem in the application of the equations presented above is the calculation of K and n . It has been shown in [7], that the method of Motzkus [19,7,41,42] (filling) and Arnold and McLean [41,7] (discharging) make possible a fairly realistic assessment of the stresses in the hopper. Since these equations are relatively complicated, they will not be presented here. In the program SSTOOL [44] the methods mentioned above are used.

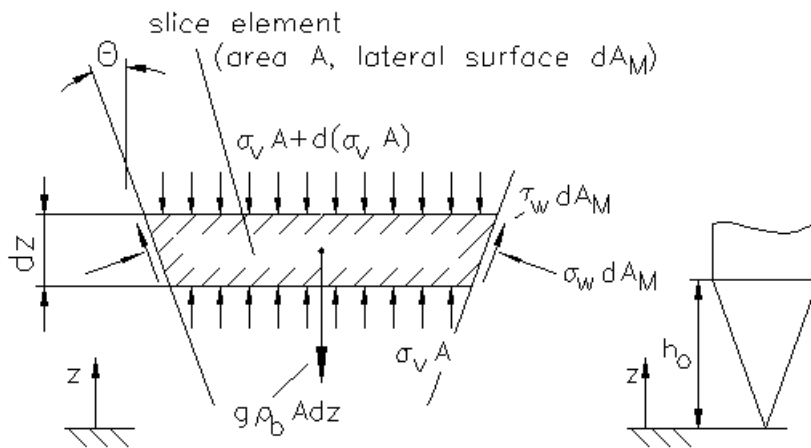


Figure 8: Slice element in the hopper

3. Irregularities

3.1 Switch

The stresses acting on the silo walls have to be known for the structural design of a silo. On one hand, these can be the stresses as described in section 2. On the other hand additional loads on the silo walls which result from, for example, non-uniform stresses across the perimeter or local stress peaks have to be taken into account.

In section 2 the stress peak which appears at the transition from the vertical section to the hopper in the passive stress field in mass flow silos was mentioned ("switch", see figure 3.c). The reason for the switch can be clarified with a consideration of plausibility: A relatively large vertical stress σ_v acts on the bulk solid in the hopper because in the vertical part of the silo the major principal stress acts downwards. In the hopper the bulk solid is compressed horizontally as it flows downwards. Therefore, in the hopper the horizontal stress is larger than the vertical stress. Due to the equilibrium of forces, the vertical stress σ_v at the upper end of the hopper is equal to the vertical stress σ_{v0} at the lower end of the vertical section. Then in the hopper axis σ_h is larger than σ_{v0} . However, at the lower end of the vertical section the horizontal stress $\sigma_h = \lambda \sigma_{v0}$ is obviously smaller than σ_{v0} . This situation explains the abrupt increase of the horizontal stress at the transition from the vertical section to the hopper. Only the stresses in the axis of the silo are included in this consideration of plausibility because

the horizontal and the vertical stresses are principal stresses only at that position. With decreasing distance to the silo walls the directions of the principal stresses are more and more sloped against the horizontal and the vertical line (see trajectories in figures 3 and 4).

The calculation of the switch stresses is possible in principle, e.g. using Enstad's method [17]. There are other approaches as well, e.g. from Walters [15,16] and Jenike [35]. New investigations apply the finite element method (FEM, e.g.[20-22]) to calculate the temporary courses of the stresses.

In the case of mass flow silos, the switch generally appears at the transition from the vertical section to the hopper. This has to be considered for the structural design [1]. In the case of funnel flow silos, however, the switch appears where the borderline between dead zones and the flowing bulk solid intersects the silo wall (figure 9.b). Because of this, the stress peak is located in the sensitive area of the vertical section on the one hand, and on the other hand the vertical position of the switch can vary along the perimeter and can also vary with time. This has to be taken account for the structural design [1]. Some bulk solids (e.g. different types of sugar), if stored in a funnel flow silo, form flow zones with nearly vertical borderlines which do not intersect the silo wall at any point. Hence, they cannot generate stress peaks on the silo wall (figure 9.a).

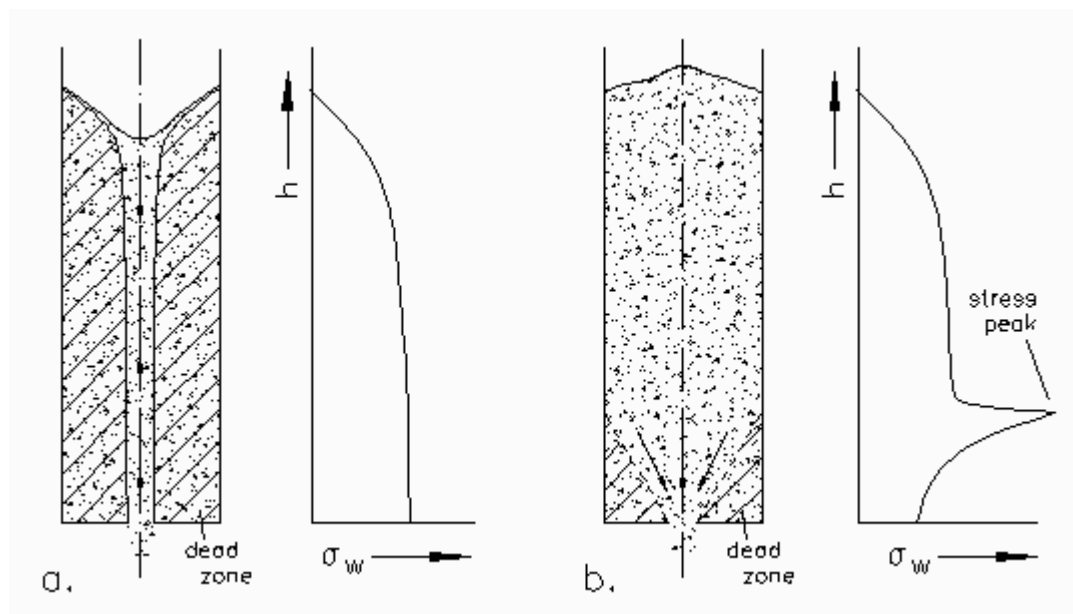


Figure 9: Wall normal stress in funnel flow silos a. steep border line b. flat border line

3.2 Imperfections

Even in mass flow silos local stress peaks in the vertical section are possible. The stress peaks are caused by irregularities (imperfections) in the silo wall [35-37], i.e. the vertical section is converging locally due to a local reduction in the cross-sectional area. Measurements taken by van Zanten and Mooij [38] on a silo with artificial imperfections in the vertical section have shown that locally the passive state of stress prevails. The wall normal stress can increase significantly in the vicinity of the

imperfections (up to four times of the horizontal stress measured without imperfections). This effect is comparable to the switch (section 3.1).

3.3 Eccentric flow

If the bulk solid in a silo does not flow downwards uniformly across the cross-section but in an eccentric flow zone, then this behaviour is called eccentric flow. Typical reasons for eccentric flow are:

- Funnel flow silo with an asymmetrically formed flow zone, especially in the case of an eccentric outlet opening.
- Silo with a feeder which withdraws the bulk solid only from a part of the outlet opening.
- Asymmetric hopper.
- Silo with more than one outlet opening of which not all are in use.

The problems of eccentric flow are, in addition to the known problems of funnel flow, the non-uniform stress distribution over the perimeter which has to be considered in structural design. Because of the non-uniform load on the silo walls, bending moments and normal forces are caused which would not occur during a regular loading.

The non-uniform stress distribution can be explained as follows. Figure 10.a shows schematically a vertical section of a silo (diameter d) from above with an assumed flow zone (diameter d_f). A longitudinal section of the silo is drawn in figure 10.b. The bulk solid in the flow zone which flows downwards affects not only the silo wall but also the bulk solid at rest (dead zone) with downwards directed shear stresses τ , i.e. the bulk solid in the flow zone transmits a part of its weight to the silo walls and to the bulk solid at rest (the shear stresses are drawn in their direction of action). Therefore, the stress in the flow zone decreases whereas the stress in the dead zone increases. In reality the situation is more complicated..

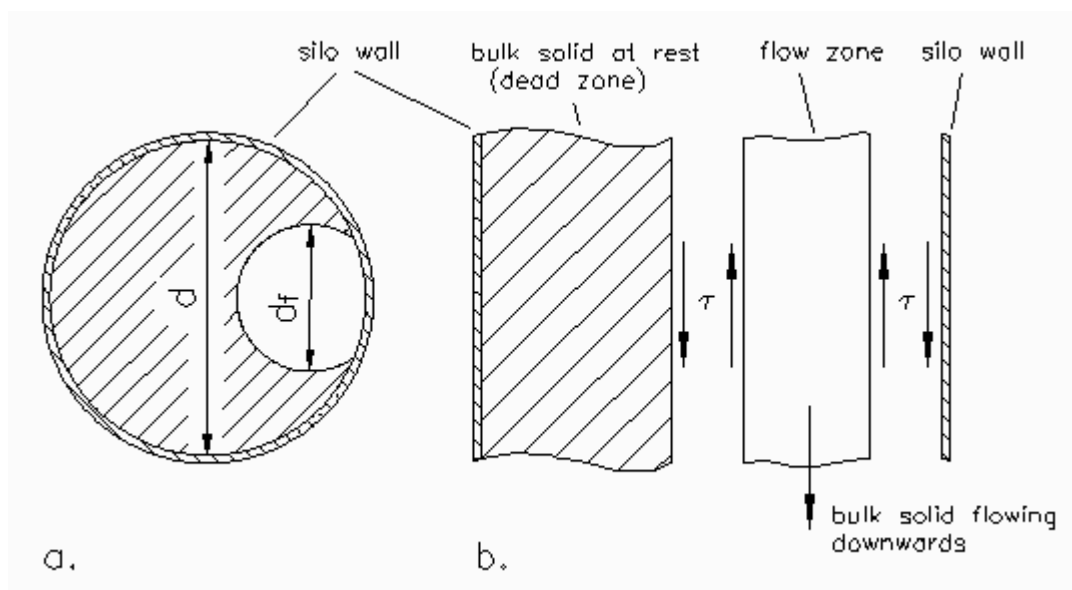


Figure 10: Eccentric flow in the vertical section of a silo (schematic) a. top view b. longitudinal section

4. Nomenclature

A	[m ²]	area
A_M	[m ²]	lateral area of slice element
D	[m]	diameter
d_f	[m]	diameter of the flow zone
F_h	[N]	feeder force
g	[m/s ²]	acceleration due to gravity
h	[m]	height
h_0	[m]	characteristic height of the hopper (from apex to transition)
h_f	[m]	filling height
K	[-]	ratio of wall normal stress to mean vertical stress in the hopper
n	[-]	characteristic value for the calculation of hopper stresses
t	[s]	time
U	[m]	perimeter
z	[m]	coordinate in the vertical direction
λ	[-]	stress ratio
μ	[-]	coefficient of friction
ρ_b	[kg/m ³]	bulk density
σ	[Pa]	normal stress
σ_h	[Pa]	horizontal stress
σ_v	[Pa]	vertical stress
σ_w	[Pa]	wall normal stress
σ_1	[Pa]	major principal stress
σ_2	[Pa]	minor principal stress
τ_w	[Pa]	wall shear stress
φ	[°]	angle of internal friction
φ_e	[°]	effective angle of internal friction
φ_x	[°]	wall friction angle
Θ	[°]	inclination of hopper walls against the vertical

5 Literature

[1] DIN 1055, Teil 6 Lasten in Silozellen, Deutsche Norm, 1987

[2] Martens, P. (Hrsg.): Silohandbuch, Wilhelm Ernst&Sohn Verlag, Berlin, (1988)

- [3] Arnold, P.C., McLean, A.G.: Improved analytical flow factors for mass-flow hoppers, Powder Technol. 15 (1976), pp. 279-281
- [4] Jenike, A.W.: Storage and flow of solids, Bulletin No 123, Utah Eng. Exp. Station, Univ. of Utah, Salt Lake City, 1970
- [5] Schwedes, J: Fließen von Schüttgütern in Bunkern, Verlag Chemie, Weinheim (1968)
- [6] Manjunath, K.S., Roberts, A.W.: Wall pressure-feeder load interactions in mass flow hopper/feeder combinations, bulk solids handling 6 (1986) 4, pp. 769-775 and 6 (1986) 5, pp. 903-911
- [7] Schulze, D.: Untersuchungen zur gegenseitigen Beeinflussung von Silo und Austragorgan, Dissertation TU Braunschweig (1991) [pdf](#)
- [8] Roberts, A.W.: Modern concepts in the design and engineering of bulk solids handling systems, TUNRA Ltd., The Univ. of Newcastle, N.S.W., Australien
- [9] Arnold, P.C., McLean, A.G.: Bulk solids: Storage, flow and handling TUNRA Ltd., The Univ. of Newcastle, N.S.W., Roberts, A.W. Australien
- [10] Janssen, H.A.: Getreidedruck in Silozellen, Z. Ver. Dt. Ing. 39 (1895), pp. 1045-1049
- [11] Koenen, M.: Berechnung des Seiten- und Bodendrucks in Silozellen, Centralblatt der Bauverwaltung 16 (1896), pp. 446-449
- [12] Jenike, A.W.: Gravity flow of bulk solids, Bulletin No 108, Utah Eng. Exp. Station, Univ. of Utah, Salt Lake City, 1961
- [13] Walker, D.M.: An approximate theory for pressures and arching in hoppers, Chem. Eng. Sci. 21 (1966), pp. 975-997
- [14] Walker, D.M.: A basis for bunker design, Powder Technology 1 (1967), pp. 228-236
- [15] Walters, J.K.: A theoretical analysis of stresses in silos with vertical walls, Chem. Eng. Sci. 28 (1973), pp. 13-21
- [16] Walters, J.K.: A theoretical analysis of stresses in axially-symmetric hoppers and bunkers, Chem. Eng. Sci. 28 (1973), pp. 779-789
- [17] Enstad, G.G.: A novel theory on the arching and doming in mass flow hoppers, Dissertation, Chr. Michelsen Inst., Bergen, Norwegen (1981)
- [18] Benink, E.J.: Flow and stress analysis of cohesionless bulk materials in silos related to codes, Dissertation, Universität Twente, Enschede, Niederlande (1989)

- [19] Motzkus, U.: Belastung von Siloböden und Auslauftrichtern durch körnige Schüttgüter, Dissertation TU Braunschweig (1974)
- [20] Häußler, U.: Geschwindigkeits- und Spannungsfelder beim Entleeren von Silozellen, Dissertation Univ. Karlsruhe (1984)
- [21] Rombach, G., Eibl, J.: Consistent modelling of filling and discharging processes in silos, Preprints "Silos - Forschung und Praxis", Karlsruhe (1988), pp. 1-15
- [22] Rombach, G.: Schüttguteinwirkungen auf Silozellen - Exzentrische Entleerung, Dissertation Univ. Karlsruhe (1991)
- [23] AS 3774-1990 Loads on bulk solids containers, Australian Standard, 1987
- [24] BMHB Draft code of practice for the design of silos, bins, bunkers and hoppers, British Material Handling Board (1985)
- [25] Hampe, E.: Silos, Band 1 (Grundlagen), VEB Verlag für Bauwesen, Berlin 1987
- [26] Pieper, E., Wenzel, F.: Druckverhältnisse in Silozellen, Verlag Wilhelm Ernst & Sohn, Berlin 1964
- [27] Wolf, K.: Der Anfangsschlag und andere Belastungsgrößen im Silo, Diss. TU Braunschweig (1984)
- [28] Kézdi, A.: Erddrucktheorien, Springer Verlag Berlin 1962
- [29] Jenike, A.W.: Storage and flow of solids, Bulletin No 123, Utah Eng. Exp. Station, Univ. of Utah, Salt Lake City, 1964 (revised edition 1970)
- [30] ISO TC98/SC3/WG5: Loads due to bulk materials (Draft), Karlsruhe, Sept. 1990
- [31] Zachary, L.W., Lohnes, R.A.: A confined compression test for bulk solids, Proc. 13th Annual Powder & Bulk Solids Conf., May 1988, Rosemont, IL, USA
- [32] Nielsen, J., Kolymbas, D.: Properties of granular media relevant for silo loads, Preprints "Silos - Forschung und Praxis", Karlsruhe (1988), pp. 119-132
- [33] Kwade, A., Schulze, D., Schwedes, J.: Die direkte Messung des Horizontallastverhältnisses Teil 1 und 2, Beton- und Stahlbetonbau 89 (1994) 3, pp. 58-63 und 89 (1994) 4, pp.117-119
- [34] Kwade, A., Schulze, D., Schwedes, J.: Determination of the Stress Ratio in Uniaxial Compression Tests Part 1 and 2, Powder Handling & Processing 6 (1994) 1, pp.61-65 und 6 (1994) 2, pp.199-203
- [35] Jenike, A.W., Johanson, J.R., Carson, J.W.: Bin loads - Part 2 and 3, Journ. of Eng. for Industry, Trans. ASME, Series B, Vol.95, No 1, Feb. 1973, pp.1-12

- [36] Stiglat, K.: Statisch-konstruktive Bemessung von Silos, Preprints der VDI-GVC-Tagung "Agglomerations- und Schüttguttechnik", Baden-Baden (1991), pp.109-138
- [37] Jenike, A.W.: Load Assumptions and distributions in silo design, Conf. on construction of concrete silos, Oslo, Norwegen, Januar 1977
- [38] Van Zanten, D.C., Mooij, A.: Bunker Design, Part 2: Wall pressures in mass flow, Journ. of Eng. for Industry, Trans. ASME, Nov. 1977, pp.814-818
- [39] Frese, B.: Druckverhältnisse in zylindrischen Silozellen, Dissertation, TU Braunschweig (1977)
- [40] McLean, A.G.: Initial stress fields in converging channels, Bulk Solids Handling 5 (1985) 2, pp. 49-54
- [41] Arnold, P.C., McLean, A.G.: An analytical solution for the stress function at the wall of a converging channel, Powder Technology 13 (1976), pp. 279-281
- [42] Schulze, D.: The prediction of initial stresses in hoppers, Bulk Solids Handling 14 (1994) 3, pp. 497-503
- [43] Schulze, D., Schwedes, J.: An examination of initial stresses in hoppers, Chem. Engng. Sci. 49 (1994) 13, pp. 2047-2058
- [44] Schulze, D.: Silo Stress Tool (SSTOOL), program for the assessment of stresses in containers and silos. Download at www.dietmar-schulze.de (1999)